Orbit jump in bistable energy harvesters through buckling level modification

Thomas Huguet, Mickaël Null Lallart, Adrien Badel

Orbit jump in bistable energy harvesters through buckling level modification

Thomas Huguet [a,b], Mickaël Lallart [a] and Adrien Badel [b,*]

[a] Univ. Lyon, INSA-Lyon, LGEF, EA682, F-69621, Villeurbanne, France

[b] Univ. Savoie Mont-Blanc, SYMME, F-74000, Annecy, France

[*] corresponding author: adrien.badel@univ-smb.fr

Abstract

In the aim of giving an alternative to chemical batteries for energy supply of wireless autonomous devices, the present work focuses on ambient vibration energy harvesting using harvesters taking benefit of energy stored in an oscillating mass subjected to acceleration. More particularly, the attention is put on nonlinear bistable harvesters which offer a wider bandwidth than linear ones. However, due to their nonlinearities, these bistable harvesters exhibit different coexisting behaviors (orbits) on their operating frequency range. Only some of them are interesting for energy harvesting because of their high amplitude of oscillations inducing high energy levels (high orbits). Nevertheless, those high orbits are coexisting with low orbits (i.e., low harvestable energy) on a major portion of their frequency range and thus are not automatically reached. This work hence introduce new strategies to experience orbit jumps from low to high orbits playing with different parameters of the bistable harvester. Preliminary analyses based on energy considerations demonstrates that the most technically achievable strategy, adopted for the experimental analysis, is the orbit jump with fast modifications of its buckling level. More particularly, the bistable harvester is first quickly over-buckled at a particular instant and then quickly released to its initial buckling level when the mass reaches a maximum of displacement (in order to maximize the potential energy brought to the mass). Two elements of this strategy were adjustable: the amplitude of the buckling level variation and the instant at which this change starts. Experimental results show that choosing a good combination of those two elements leads to a high probability to jump from low to high orbits on the whole frequency range concerned by high orbits (from 70% chance to 100% chance to jump). Thanks to this orbit jump technique, the high orbits can be ensured for the considered bistable harvester on a continuous wide frequency range of 50 Hz (from 20 Hz to 70 Hz) on which the mean harvested power varies from 20 μW to 500 μW. Finally, it is shown that the energy consumed to ensure the orbit jump can be recovered within 2 seconds.

I. Introduction

The current interest for energy harvesting is clearly linked to the growing number of stand-alone, left behind, wireless devices in all the industrial fields as well as in consumer electronics domain. Such a concern is explained by the fact that primary batteries used to ensure the energy needs have a limited autonomy that may be lower than the life time of the devices, especially when the latter experience relatively harsh conditions (*e.g.*, temperature). Among other energy sources surrounding the system, vibration energy harvesters have been proposed to give an alternative to those primary batteries able to work in indoor and confined environments, where photovoltaic cells cannot be used for instance. More particularly inertial harvesters have been highlighted [1] for their easiness of implementation on different vibrating structures. Although these inertial harvesters allow an amplification of the vibrations at their natural frequency [2], their main limitation remains their narrow frequency bandwidth which is not acceptable for non-constant or random vibrations. Nonlinearities have therefore been intentionally brought into the behaviors of such inertial harvesters to enhance their frequency bandwidth such as bistable harvesters [3–7].

However these nonlinearities have another side effect. Several different behaviors can coexist on the same frequency range, solely determined by its initial conditions. Some of those behaviors are interesting for energy harvesting, namely the common harmonic 1 high orbit (for which the mass moves from one stable position to another at the same frequency as the excitation) [8, 9] and the subharmonic 3 high orbit (for which the mass moves from one stable position to another at a frequency 3 times lower than the excitation), as reported by the authors in previous studies [10, 11]. However, some other behaviors, namely the low orbits (for which the mass oscillate around one stable position), are not interesting for energy harvesting as they induce low amplitude displacements and thus low energy levels. As the steady-state behavior reached by the nonlinear harvester is uncertain in real conditions, a strategy has to be found to allow jumps from low to high orbits, hence ensuring optimal operating conditions.

A few strategies for orbit jumps have already been studied in the literature. The first strategy is to bring a disturbance to the nonlinear harvester when it is on a low orbit to create the jump. Proofs of this concept have been brought by Erturk *et al.* [12] with a hand impulsion or by Wu *et al.* [13] and Lan *et al.* [14] with an electrical pulse

disturbance applied on the transducer (piezoelectric or magnetic). Then Zhou *et al.* [15] did a numerical and experimental investigation of this concept with a projectile impacting the mass showing the possibility to jump from low to high orbits. Another strategy have been proposed by Sebald *et al.* [16, 17] which consists of exciting the piezoelectric transducer with a sinusoidal voltage on several cycles (from 1 to 20). This strategy, called Fast Burst Perturbation (FBP), creates a new excitation which adds to the vibration source to force the system to stabilize on a high orbit. Masuda *et al.* [18] proposed a similar strategy. They also add a parallel excitation to their transducer but through a negative resistance which acts as a negative damping. This negative resistance is plugged each time the three last peaks of the mass displacement are below a certain threshold. Udani *et al.* [19] and Mallick *et al.* [20] also experimented the concept of adding a parallel artificial excitation to the vibration source with a new approach, considering a phase shift of the resulting excitation (the source plus the parallel excitation) compared to the vibration source on several cycles leading to jump from low to high orbits. This strategy has the advantage to be deterministic as the successful phase shift can be obtained calculating the basins of attraction of the harvester (orbits reached according to its initial conditions) as a function of the excitation phase shift [19]. Finally, a strategy called stochastic resonance has been investigated in particular by Dykman *et al.* [21] and Almog *et al.* [22] allowing orbit jumps through the addition of a white noise to the low orbits. Nevertheless, all these proofs of concept rarely precise the jump probabilities offered by these strategies over the whole frequency range of the harvester.

This article proposes an analysis as well as a full experimental study of an efficient approach to jump from low to high orbits, which will be characterized by its efficiency in terms of jump probabilities and in terms of energy cost over the entire frequency range of the bistable harvester. The orbit jump is here investigated through the modification of the parameters of the bistable harvester (stiffness and buckling level), and more particularly with its buckling level. First the bistable harvester equations governing its behavior are introduced, leading, after a resolution with harmonic balance method, to frequency responses which highlight all the different steady-state behaviors of the bistable harvester with respect to the excitation frequency. Then, different strategies to experience orbit jumps from low to high orbits through the modification of different parameters of the bistable harvester are devised. The most technically achievable strategy adopted for the experimental analysis is orbit jump using the buckling level. The optimization of this strategy is then conducted analyzing the effects of the different adjustable elements, namely the amplitude of the buckling variation and the instant at which this change starts. The experimental results show that choosing a good combination of those two elements leads to a high probability to jump from low to high orbits on the whole frequency range concerned by high orbits (from 70% to 100% probability to jump, depending on the excitation frequency). Thanks to this orbit jump technique, the high orbits can be ensured for the bistable harvester used in our experiments on a continuous wide frequency range of 50 Hz (from 20 Hz to 70 Hz), hence ensuring optimal energy harvesting operations.

II. Bistable harvester behaviors and their associated stability robustness

This section introduces the bistable harvester studied in this article as well as the equations governing its behavior. The bistable harvester analytical frequency response is introduced highlighting all the different steady-state behaviors with respect to the excitation frequency.

The bistable harvester model used in this article is depicted in Figure 1. The displacement x of the mass M is defined with respect to the frame. At equilibrium, the mass displacement can take one of the two stable values referred as $\pm x0$. Under such conditions, the length between the frame and the center of the mass is annotated L as shown in Figure 1. The frame is linked to an external excitation source which imposes a sinusoidal acceleration of amplitude A and angular frequency ω. A piezoelectric transducer is used to ensure the conversion from mechanical energy to electrical energy. Piezoelectric transducers are commonly modeled as two different parts working in parallel: a spring k_{piezo} and an element ensuring the energy conversion defined by its force factor α and its capacitance C_0. A resistance R is connected to the transducer to account for the energy harvesting circuit. The electrical energy transferred to the resistance, dissipated by Joule effect, corresponds to the entire energy converted from the excitation source and is calculated by integrating the squared resistance voltage v divided by R. To maximize this harvested energy, the resistance has been set to match the internal impedance of the piezoelectric element $R = 1/C_0\omega$.

To describe the bistable harvester, two equations are used: a Duffing-type mechanical equation and the electrical equation. Those two equations are coupled by the

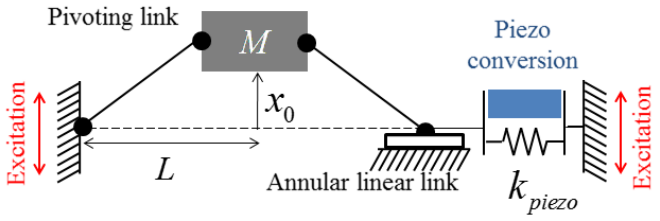

Figure 1: *Design of the bistable harvester principle (here shown in one of its stable position).*

piezoelectric effect:

$$\begin{cases} \ddot{x} + \dfrac{\omega_0^2}{2}\left(\dfrac{x^2}{x_0^2} - 1\right)x + \dfrac{\omega_0}{Q}\dot{x} + \dfrac{2\alpha}{ML}xv = -A\cos(\omega t) \\ C_0\dot{v} = 2\dfrac{\alpha}{L}x\dot{x} - \dfrac{v}{R} \end{cases} \tag{1}$$

As defined by Liu et al. [23], ω_0 and Q respectively refer to the natural angular frequency and the mechanical quality factor of the equivalent linear oscillator obtained for small excitation inducing small displacements of the mass near one of the stable positions ($x = \pm x_0 + \Delta x$ with $\Delta x << x_0$). The parameters of the bistable harvester mentioned above are summarized in Table 1. Their values correspond to the prototype used in the experimental analysis.

Equation (1) is analytically solved with the harmonic balance method (including harmonic 1 response and subharmonic responses) for different excitation angular frequency ω to obtain the bistable harvester frequency responses highlighting all its steady-state behaviors (or orbits) with respect to the excitation frequency. For each found behavior, a stability analysis is conducted with the small disturbance method thanks to the Floquet theory and the Lyapunov exponents (*i.e.*, the most popular approach; for a review of this technique, the reader can refer to the work of Friedmann [24]). As the equations are nonlinear, multiple steady-state behaviors can coexist for the same excitation amplitude and frequency and for a given set of parameters. Some of them are depicted in Figure 2 for parameters listed in Table 1. For each of them, a time signal is presented as well as a phase portrait for different excitation frequencies. The steady-state behaviors highlighted in Figure 2 are those the authors

Table 1: *Parameter values of the bistable harvester corresponding to the experimental prototype.*

Parameter	Symbol	Value	Unit
Stable positions	$\pm x_0$	± 0.50	mm
Mass-frame distance	L	25	mm
Inertial mass	M	17.3	g
Natural angular frequency	ω_0	121	rad.s^{-1}
Mechanical quality factor	Q	87	–
Excitation magnitude	A	2.5	m.s^{-2}
Excitation frequency	ω	$15 - 85$	Hz
Piezoelectric force factor	α	0.068	N.V^{-1}
Piezoelectric blocked capacity	C_0	1.05	μF
Load resistance	R	7.83	kΩ

reported as an interesting aspect for energy harvesting purpose in a previous work [10], namely the common harmonic 1 orbit and the subharmonic orbits. Subharmonic orbits are defined as follow: for subharmonic n orbit, the mass moves with a frequency n times lower than the excitation frequency.

Moreover the high orbits defined as stable with the small disturbance method are not all equivalent. On some frequency ranges, some of them are easier to reach and maintain over time (*i.e.*, without following on a low orbit) because they are less sensitive to external disturbances. Those orbits, defined on restricted frequency ranges, are more interesting for energy harvesting as they are more suitable in realistic conditions. To estimate this sensitivity to external disturbances, the authors recently introduced an analytic criterion called the stability robustness [11] that will be used through this study.

The idea of the stability robustness analysis is to disturb the stable high orbits with a pulse and to analytically

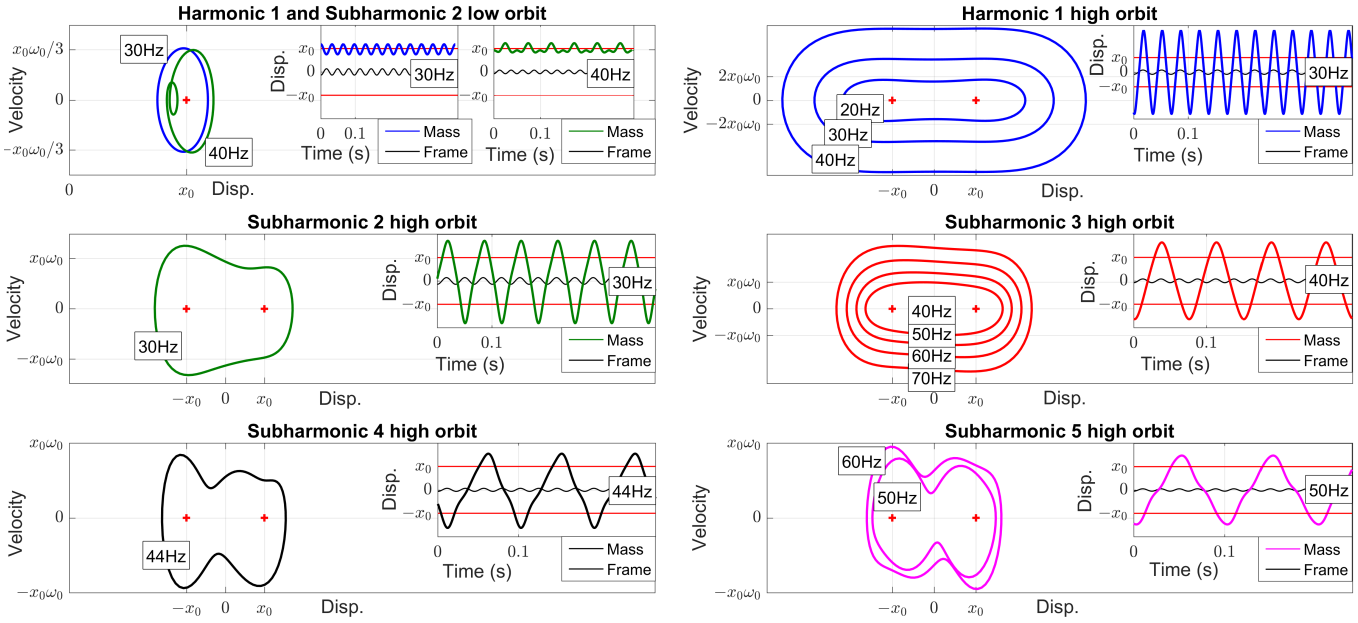

Figure 2: *Phase portraits and time signals of different steady-state behaviors (or orbits) of the bistable harvester including subharmonic orbits (for subharmonic n orbit, the mass moves with a frequency n times lower than the excitation frequency). Those behaviors have been analytically found resolving Equation (1) for several excitation frequencies. A unique color has been used for each kind of behavior: harmonic 1 orbits in blue, subharmonic 2 orbits in green, subharmonic 3 orbits in red, subharmonic 4 orbits in black and subharmonic 5 orbits in pink.*

determine the lowest pulse needed to destabilize them (*i.e.*, the lowest pulse making the high orbits jump on low orbits). The greater the energy of the lowest pulse needed to destabilize the orbit, the more robust the orbit. Hence, the stability robustness criterion for stable high orbits is defined as the energy of the lowest pulse needed to destabilize them normalized by the energy provided by the excitation to the mass per cycle. For low stability robustness, the stable high orbits will no longer be considered as interesting for energy harvesting because too sensitive to disturbances for being maintainable over time.

Figure 3 shows the bistable harvester analytical frequency responses obtained with the parameters listed in Table 1 and following the procedure detailed in [11]. Four different spectra are presented: the amplitude of stable orbits, the phase of the excitation displacement when the position of the mass reaches a maximum for stable high orbits, the stability robustness for stable high orbits, and the mean harvested power for stable orbits. The stability robustness threshold defines the minimum stability robustness needed to consider the high orbits as robust enough for energy harvesting, and has been determined experimentally as it will be exposed later.

Figure 3(a) shows a spectrum rich in behaviors. The low orbits (or intra-well motions) and the high orbits (or inter-well motions) have amplitude respectively lower and bigger than x_0. For high orbits, we arbitrary stopped the analytical analysis at subharmonic 5 because subharmonic orbits of higher order are less interesting for energy harvesting (their amplitudes are small compared to the subharmonic orbits presented and their frequency ranges does not help in widening the bandwidth of the bistable harvester).

Similarly, we stopped the analytical analysis of low orbits at subharmonic 2, as such low orbits are not of interest for energy harvesting purposes. Some low orbits are however considered here as reference to know the frequency ranges on which high orbits does not exist alone and could consequently jump down on a low orbit. More particularly, low orbits introduced in Figure 3(a) are those which increase the total frequency range of such low orbits.

The robustness stability shown in Figure 3(c) confirms the experimental observations: the stable high orbits are not all equally sensitive to external disturbances and are thus more or less easy to maintain over time (making them more or less interesting for energy harvesting). It can be noted that the stability robustness of even subharmonic high orbits is low compared to odd subharmonic high orbits which confirms the difficulty of observing them experimentally. The stability robustness of harmonic 1 and odd subharmonic high orbits decreases as they approach their theoretical cutting frequency happening when the phase shown in Figure 3(b) reaches $\pi/2$ [11, 25]. It is interesting to note that the frequency

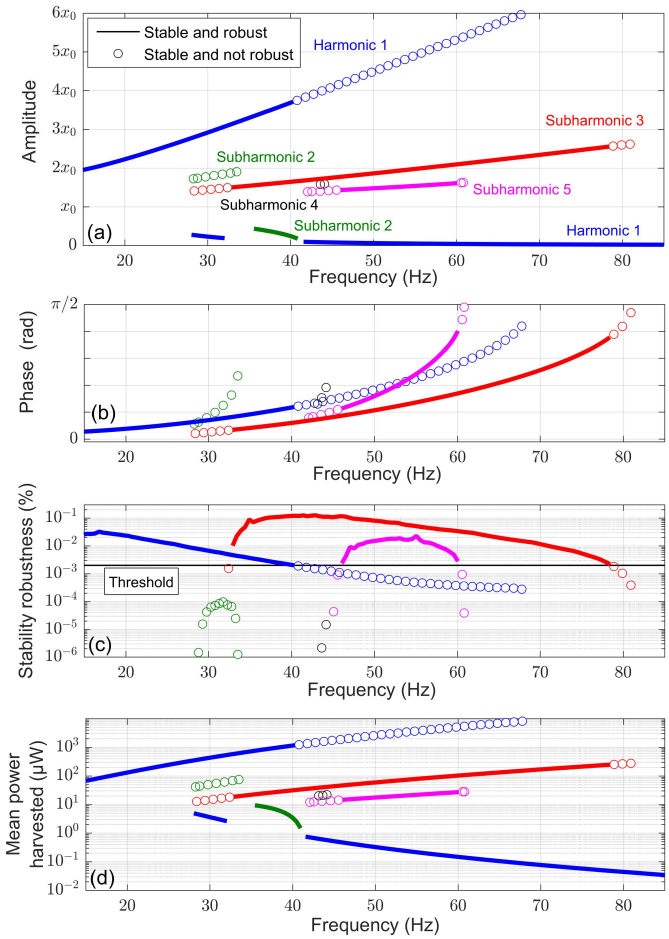

Figure 3: *Bistable harvester spectra analytically obtained for a sinusoidal acceleration of magnitude 2.5 m/s^2: (a) amplitude of stable orbits (b) phase of the excitation displacement when the position of the mass reaches a maximum for stable high orbits (c) stability robustness for stable high orbits (d) average harvested power for stable orbits. A unique color has been used for each kind of behavior: harmonic 1 orbits in blue, subharmonic 2 orbits in green, subharmonic 3 orbits in red, subharmonic 4 orbits in black and subharmonic 5 orbits in pink.*

range of the common harmonic 1 high orbit is not as wide as the classic analytical analysis would let believe. Its frequency range is divided by 2 when the stability robustness analysis is taken into account. On the opposite, subharmonic 3 high orbit is more robust and its frequency range is less affected. Subharmonic 3 orbit then appears to be relevant for energy harvesting purposes as it greatly enhances the frequency range on which the bistable harvester proposes a high orbit, as reported in [11].

III. Orbit jump strategies playing with bistable harvester parameters

Figure 3 shows promising theoretical results for the bistable harvester which has a continuous frequency band of 63 Hz (from 15 Hz to 78 Hz) for which a robust high orbit exists making it ideal for real condition wideband vibration energy harvesting as it can be adapted to non-constant vibrations. However, those high orbits

are coexisting with low orbits (*i.e.*, low harvested energy) on a major portion of their frequency range and are thus not automatically reached. This section investigates different strategies to experience orbit jumps from low to high orbits. These orbit jumps are obtained playing with different parameters of the bistable harvester and will ensure that the bistable harvester reaches a high orbit in real conditions whenever it is possible.

The idea of the orbit jump strategies is to somehow provide energy to the mass through the modification of one parameter of the bistable harvester. The equations describing the bistable harvester detailed in Equation (1) exhibit five different mechanical parameters: (M, x_0, L, ω_0, Q) which are respectively the mass; the mass equilibrium position; the length between the frame and the center of the mass at equilibrium; the natural angular frequency and the mechanical quality factor of the equivalent small excitation linear oscillator. The modification of the mass M or the quality factor Q during the experiment have been considered as less technically achievable (energy consuming approaches). Those two parameters have therefore not been kept. Then, a change in the length L induces a change in the equilibrium position x_0 so modifying any of these two parameters is equivalent. Finally, the only way to change ω_0 without modifying the mass M or the length L, is to tune the stiffness of the piezo k_{piezo}.

In conclusion, two different parameters have been preselected to provide energy to the mass in order to experience orbit jumps: the length L between the frame and the center of the mass at equilibrium and the stiffness of the piezo k_{piezo}. Those two parameters are visible in Figure 1. Figure 4 shows the principles of the two strategies used to provide energy to the mass with these two parameters. Time signals numerically obtained are presented. The parameters used for these numeric simulations are those listed in Table 1.

The strategy to provide energy to the mass changing L is as follows. As shown in the example of Figure 4(a), the mass is numerically stabilized on the harmonic 1 low orbit with an excitation frequency of 50 Hz and an excitation amplitude of 2.5 m/s^2. Then the length L is reduced by 0.02% inducing an increase of the buckling level which corresponds to an increase of $|x_0|$. As shown in Figure 4(b), this operation, supposed to be instantaneous, increases the elastic potential energy of the system as the distance between the mass position and $|x_0|$ increases. The length L is maintained reduced until the position of the mass reaches a maximum. Then the length L is brought back to its initial value which induces a decrease of the buckling level and $|x_0|$ to their initial values. This operation, also supposed to be instantaneous, increases again the elastic potential energy of the system as the distance between the mass position and $|x_0|$ increases again. The instant chosen for this second operation (*i.e.*, when the position of the mass reaches a maximum) is set to maximize the potential energy provided to the mass. Indeed, this instant ensure that the distance between the mass position and $|x_0|$ is increased as much as possible when the length L is brought back to its initial value. In the example shown in Figure 4(a) and (b), the total potential energy provided to the mass through the modification of the length L is 30 μJ.

The strategy to provide energy to the mass changing k_{piezo} is as follows. Similarly as the previous strategy the mass is numerically stabilized on the harmonic 1

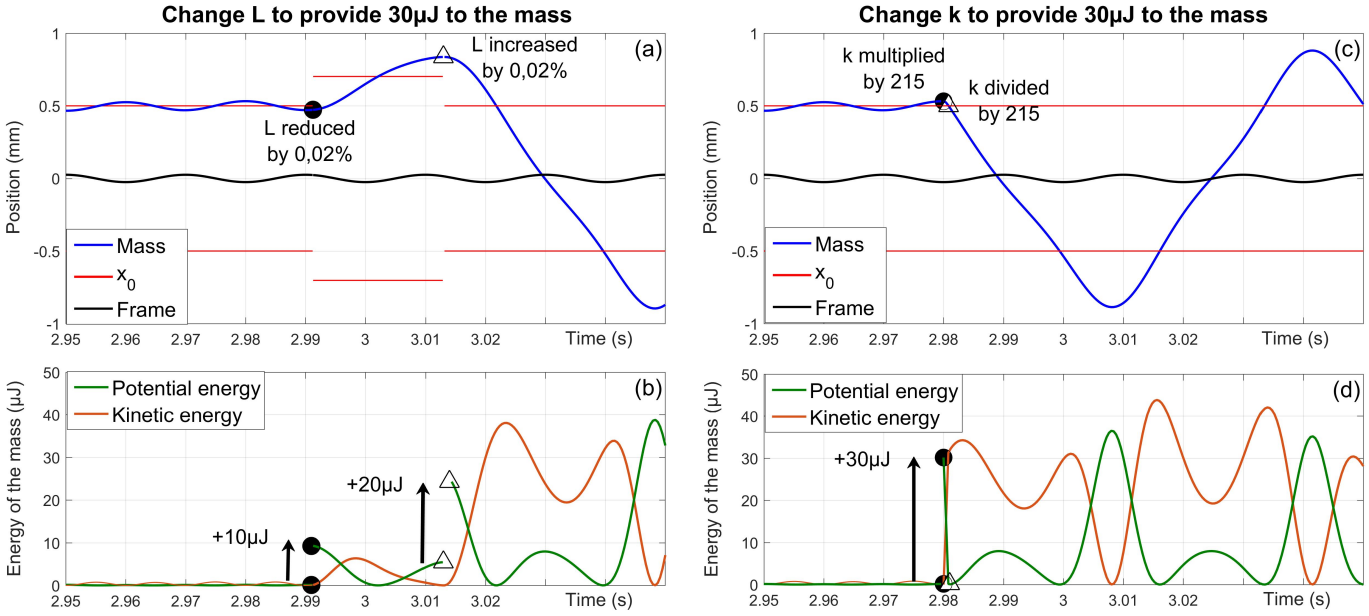

Figure 4: *Numerical example time signals introducing two different strategies to provide a certain amount of energy (here 30 µJ) to the mass by modifying the length L or the stiffness k_{piezo} of the bistable harvester in order to experience orbit jumps. More particularly, these two strategies are intended to provide 30 µJ of potential energy to the mass. For each strategy two time signals are introduced: (a) and (c) the mass displacement; (b) and (d) the potential and kinetic energy of the mass.*

low orbit with an excitation frequency of 50 Hz and an excitation amplitude of 2.5 m/s^2 (Figure 4(c)). Following Equation (1, it can be shown that the elastic potential energy of the system is directly proportional to k_{piezo} therefore, multiplying k_{piezo} leads to multiply the elastic potential energy with the same factor. In order to maximize the energy provided to the system changing k_{piezo}, the latter is multiplied when the elastic potential energy of the system reaches a maximum so when the mass position reaches a maximum. Then k_{piezo} is kept as is until the elastic energy of the system is zero, where k_{piezo} is finally brought back to its initial value. This last operation does not reduce the energy of the system. In the example shown in Figure 4(c) and (d), k_{piezo} is multiplied by 215 and then divided by 215. Similarly to previous strategy the total potential energy provided to the mass in this example playing with k_{piezo} is 30 μJ.

Although those two different strategies both manage to provide 30 μJ to the mass, they are not all equal in terms of technical achievability. Indeed, while the change of length L of 0.02% is reachable, the multiplication of k_{piezo} by 215 seems to be unrealistic.

IV. Experimental analysis: orbit jump modifying the buckling level

The strategy adopted for the experimental analysis is the orbit jump through the modification of the length L as previously detailed in previous section and in Figure 4(a) and Figure 4(b). This section introduces the experimental prototype and the experimental setup used to investigate this strategy. Two elements of this strategy are adjustable: the amplitude of the change of length L and the instant at which this change starts. The results showed that choosing a good combination of those two elements leads to a high probability to jump from low to high orbits on the whole frequency range concerned by high orbits (from 70% to 100% probability to jump depending on the excitation frequency).

IV.1. Experimental setup and identification

Figure 5 shows the design of the bistable harvester prototype used in this experimental analysis. It is composed by two separated units: (i) the mass, the beams and the first piezoelectric transducer referred as *Piezo harvester* and (ii) the second piezoelectric transducer referred as *Piezo L modifier*. The first unit is the bistable harvester strictly speaking that is the object of this study. It is equivalent to the design introduced in Figure 1. Its parameters are listed in Table 1 and its theoretical behaviors previously described in Figure 2 and Figure 3. The two couples of two beams on each side of the mass were used to prevent the mass from rotating along the horizontal axis. The role of the second unit composed by the *Piezo L modifier* is to allow occasional modifications of the length L without interfering with the first unit during the steady-states. In other words, the *Piezo L modifier* does not affect the behavior of the bistable harvester except at particular instants when it fast changes the length L in a transient fashion. To make sure that there is no interference between the two units, the stiffness of the *Piezo L modifier* have been chosen much larger than the one of the *Piezo harvester* (5.4 times larger). It can be noted that the addition of this actuator is one solution among others to be able to modify the buckling level of the generator (proof of concept). However, the actual optimization of the buckling level modification technique is out of the scope of the present study, that focuses on the elastic potential energy that must be brought to the mass.

Figure 6 shows the bistable harvester prototype as well as the experimental setup. The mass, the frame and the beams were obtained cutting a one-piece block of APX4 steel by electric discharge machining. The different rotational links are performed using the flexibility of the thin beams (flexible connections). The prototype is buckled thanks to a nut which, when screwed, produce a translation of the screw linked to the *Piezo L modifier* toward the mass. The *Piezo harvester* and the *Piezo L modifier* are two piezoelectric actuators from Cedrat Technologies called APA (Amplified Piezoelectric Actuator), APA120S and APA100M respectively. Those actuators, visible in Figure 6, are composed of two elements: an elliptical shell of stainless steel and a preloaded stack of interdigitated piezoelectric ceramics inserted on the long axis of this shell. The elliptical shape of the shell is here used as a mechanical transformer. It amplifies along its long axis the forces applied along its short axis. On the opposite, it reduces along its long axis the deformations applied along its short axis. These APA actuators allow a better adaptation to piezoelectric ceramics which can handle strong forces but small deformations. Due to their design, these APA can only be actuated from -20V to +150V. To be able to actuate the *Piezo L modifier* on a symmetrical voltage range (from -85V to +85V), a constant bias of +65V is kept to its terminals. In the following, all the

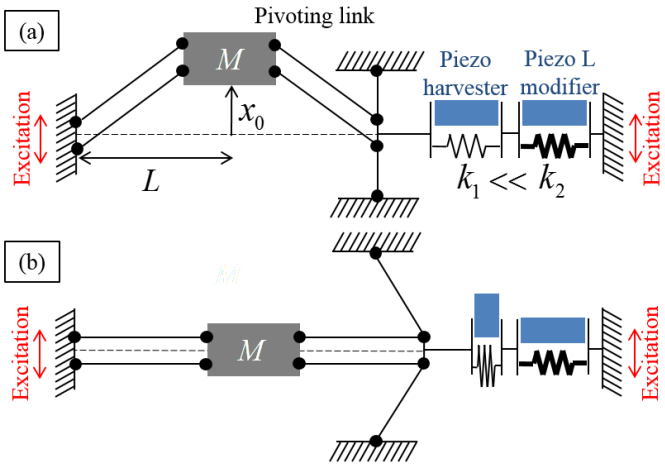

Figure 5: *Design of the bistable harvester prototype: (a) shown for one of its stable equilibrium position $x = x_0$ and (b) shown for the unstable equilibrium position $x = 0$.*

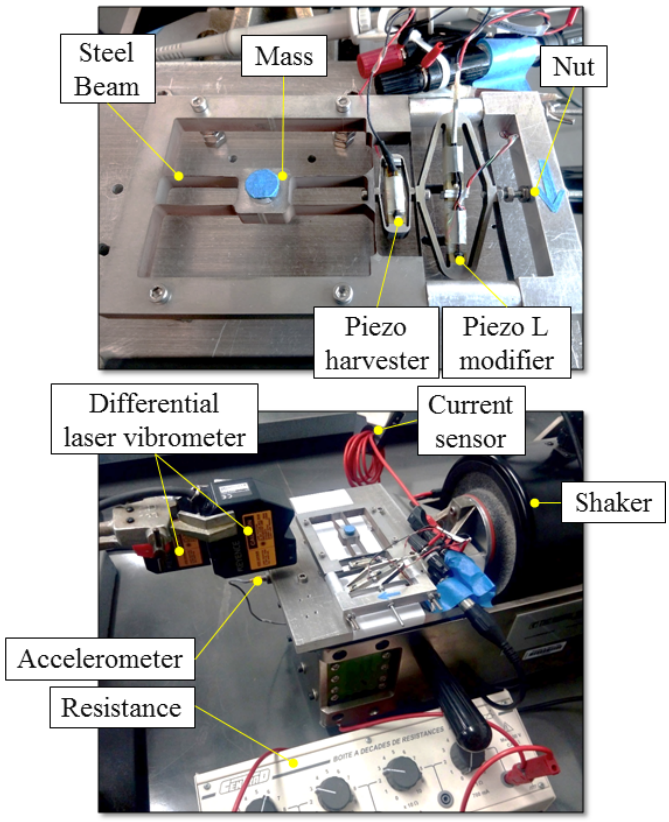

Figure 6: *Bistable harvester prototype and experimental setup.*

Table 2: *Bistable harvester prototype main dimensions.*

Elément	Value	Unity
Inertial mass (+ the blue feature)	17.3	g
Inertial mass dimensions	$16 \times 16 \times 8.0$	mm^3
APX4 steel block thickness	8.0	mm
Steel beams thickness	0.070	mm
Horizontal beams length	25	mm
Vertical beams length	17	mm

voltages applied to the *Piezo L modifier* will be expressed with respect to this bias. The main dimensions of the prototype are summarized in Table 2.

The experimental setup is composed by a shaker which imposes to the prototype an external sinusoidal acceleration of magnitude 2.5 m/s^2 at different frequencies. This excitation is measured by an accelerometer to guarantee, through a feedback loop, the desired level. The displacement of the mass with respect to the frame is measured with a differential laser vibrometer. The resistance connected to the *Piezo harvester* has been set to match its internal impedance at ω_0 ($R = 1/C_0\omega_0$) to optimize the energy conversion. The dissipated heat by the resistance through Joule's effect corresponds to the entire energy harvested from the excitation source and is calculated integrating the squared resistance voltage v divided by R. The *Piezo L modifier* is driven by a real time controller through a power amplifier. The current provided to this actuator is measured with a current sensor.

The parameters $(\omega_0, Q, C_0, \alpha)$ were identified following the procedure developed by [26]. It consists of measuring the complex admittance of the *Piezo harvester* around the natural frequency of the bistable harvester without any external excitation. This experimental admittance is then used to fit the following model:

$$\begin{cases} \underline{Y} = \dfrac{\underline{I}}{\underline{V}} = jC_0\omega \left(1 + \dfrac{k_m^2}{1 - (\omega/\omega_0)^2 + j\dfrac{\omega/\omega_0}{Q}} \right) \\ k_m^2 = 4 \left(\dfrac{x_0}{L} \right)^2 \dfrac{\alpha^2}{MC_0\omega_0^2} \end{cases} \quad (2)$$

Figure 7 shows the measurement of the prototype admittance as well as the fitted model allowing the identification of parameters $(\omega_0, Q, C_0, \alpha)$. The identified values are detailed in Table 1. Finally, the stability robustness threshold has been set to fit the upper limits of the different high orbits frequency ranges.

Figure 8 shows the frequency responses obtained experimentally with the bistable harvester prototype for a sinusoidal acceleration of magnitude 2.5 m/s^2 and compared to the analytical frequency responses previously computed. The methodology applied to obtain the frequency ranges of the different behaviors of the bistable harvester is the following: (i) set the excitation frequency for which the behavior under study is theoretically the most robust; (ii) if the behavior under study is a high orbit, apply voltage rectangular pulses of 20 ms and 30 V to the *Piezo L modifier* until it is reached; (iii) change slowly and smoothly the excitation frequency up and down until the limits of the orbit frequency range are reached; (iv) for each new frequency, wait to obtain steady-state conditions and measure three data: the excitation signal, the mass displacement with respect to the frame and the voltage across the resistance.

Hence, it can be noticed that the experimental results

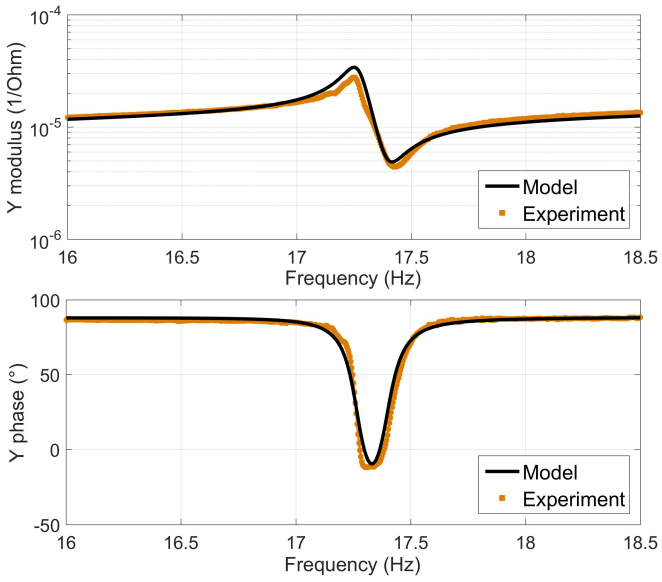

Figure 7: *Magnitude and phase of the prototype admittance and its fitted model for the identification of parameters* $(\omega_0, Q, C_0, \alpha)$.

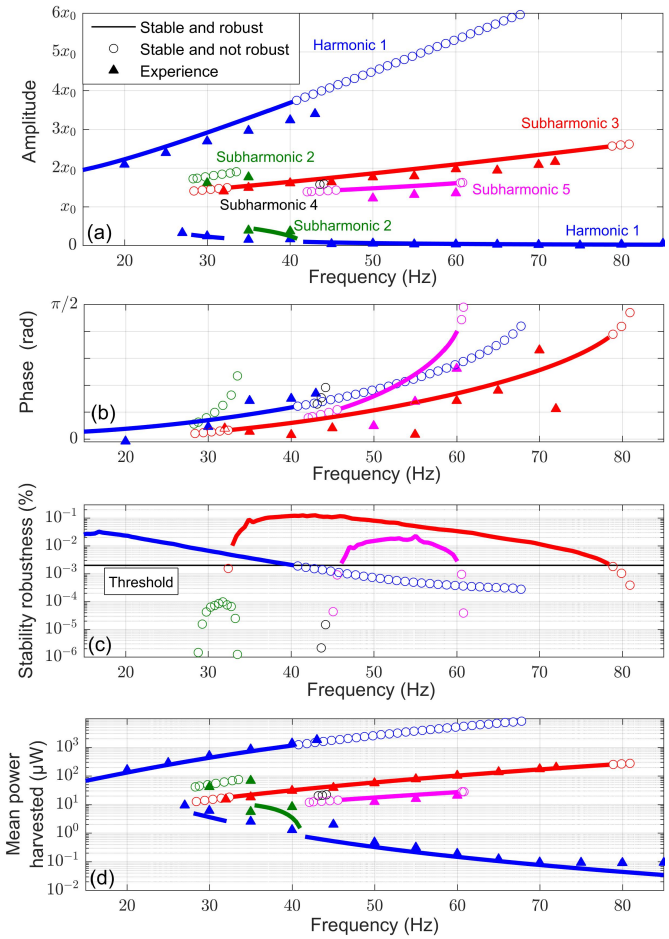

Figure 8: *Bistable harvester analytical and experimental spectra obtained for a sinusoidal acceleration of magnitude 2.5 m/s^2: (a) amplitude of stable orbits (b) the phase of the excitation displacement when the position of the mass reaches a maximum for stable high orbits (c) stability robustness for stable high orbits (d) average harvested power for stable orbits. A unique color has been used for each kind of behavior: harmonic 1 orbits in blue, subharmonic 2 orbits in green, subharmonic 3 orbits in red, subharmonic 4 orbits in black and subharmonic 5 orbits in pink.*

show good agreement with the analytical frequency responses from identified parameters once the criterion of stability robustness introduced in [11] is added, which confirms its relevance. This therefore confirms the proposed model as well as the identification procedure.

IV.2. Methodology and results

The experimentally investigated strategy to jump from low to high orbits is the orbit jump through the modification of the length L as detailed in Section III (Figure 4(a) and (b)). Two elements are adjustable: the amplitude of the change of length L and the instant at which this change starts.

Figure 9 shows an experimental measurement example while applying the change of length L. First the bistable harvester is stabilized on a low orbit. Then a negative voltage is applied to the *Piezo L modifier* which creates an elongation of this piezoelectric actuator yielding a reduction of length L. This reduction leads to further buckle the bistable harvester increasing $|x_0|$. The voltage applied to the *Piezo L modifier* can be set to start at four different instants (shown with black dots on Figure 9 and called over-buckling instants): (i) when the mass displacement reaches a maximum; (ii) when the mass displacement reaches a minimum; (iii) when the mass position is x_0 with a positive velocity; (iv) when the mass position is x_0 with a negative velocity. Then the voltage applied to the *Piezo L modifier* is set to end when the mass displacement reaches a maximum (shown with a black triangle on Figure 9). The length L is therefore increased back to its initial value leading to decrease the buckling level of the bistable harvester decreasing $|x_0|$ to its initial value. The instant of over-buckling release has been chosen to maximize the distance between the mass position and the final $|x_0|$ in order to maximize the potential energy provided to the mass during this operation.

The reduction of length L is proportional to the value of the negative voltage applied to the *Piezo L modifier*. Six different values have been studied: -20V, -30V, -40V, -50V, -60V and -70V. The orbit jumps from low to high orbits playing with the length L have been investigated for six different excitation frequencies covering all the frequency ranges of the high orbits: 30Hz, 35Hz, 40Hz, 50Hz, 60Hz

Table 3: *Adjustable elements in the experimental investigation of the strategy to jump from low to high orbits playing with the length L. The voltages applied to the Piezo L modifier are expressed with respect to the +65V bias.*

Adjustable elements	**Values investigated**
Over-buckling instants (mass condition)	maximum position minimum position x_0 with a positive velocity x_0 with a negative velocity
Voltages applied to the *Piezo L modifier*	−20V −30V −40V −50V −60V −70V
Excitation frequencies	30Hz 35Hz 40Hz 50Hz 60Hz 70Hz
Orbit jump trials for each combination	30

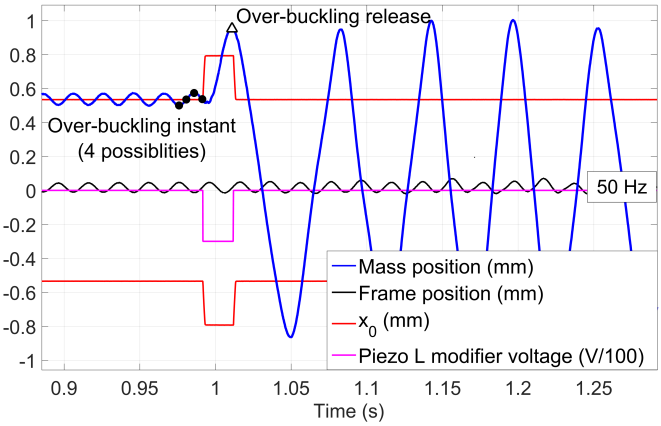

Figure 9: *Experimental time signal example of an orbit jump trial by modifying the length L (i.e, the buckling level).*

and 70Hz. All those adjustable elements are summarized in Table 3. For each possible combination, 30 orbit jump trials have been made. Each jump trial started with a steady-state harmonic 1 low orbit.

Figure 10 shows the raw data obtained during the experiments. The figure is split into four different subplots giving the results for the four different over-buckling instants (shown with black dots on Figure 9). In each subplot, the analytical frequency response is recalled as reference (thick lines and dots corresponding to stable orbits that are respectively robust and not robust). For each investigated excitation frequency, boxes are placed vertically on the subplot. Each box represents a possible steady-state behavior found after an orbit jump trial at that particular frequency. The vertical position of the box corresponds to the amplitude of the mass measured for this possible steady-state behavior. For example, Figure 10(a) shows the results for an over-buckling instant set when the mass position reaches a maximum (during the initial low orbit). For an excitation frequency of 60 Hz, 30 orbit jump trials were made for each of the six different voltages applied to the *Piezo L modifier*. After all these 180 trials, three different steady-state behaviors were found: harmonic 1 low orbit, subharmonic 5 high orbit and subharmonic 3 high orbit. These three different behaviors are represented by three boxes vertically placed at 60 Hz at their respective amplitudes.

In each box, six colored sticks are drawn standing for the six different voltages applied to the *Piezo L modifier*. The height of these sticks corresponds to the number of trials leading to the final steady-state behavior given by the position of the box. The bottom of the box corresponds to 0 trial and the top of the box corresponds to 30 trials (*i.e.*, 0% and 100% of the trials). For example, in Figure 10(a) for an excitation frequency of 60 Hz and for a -20 V *Piezo L modifier* input, the 30 trials finished on the harmonic 1 low orbit. For a -30 V input, 23 trials finished on the harmonic 1 low orbit and 7 trials finished on the subharmonic 5 high orbit. For a -40 V input, 19 trials finished on the harmonic 1 low orbit and 11 trials finished on the subharmonic 3 high orbit.

IV.3. Discussion

Several points can be noted about the orbit jumps modifying the length L from Figure 10.

(i) It is globally difficult to jump from low to high orbits. The majority of the orbit jump trials finish on a low orbit.

(ii) Those results are in good agreement with the stability robustness criterion presented in Figure 8. Indeed, among the trials finishing on a high orbit, the majority is located in high stability robustness areas (*i.e.*, between 40 Hz and 50 Hz for subharmonic 3 orbit). Moreover, there are only few trials finishing on orbits with a low stability robustness (*i.e.*, subharmonic 2, 4 and 5 high orbits).

(iii) Putting the highest possible voltage on the *Piezo L modifier* is not sufficient to experience orbit jumps. For example, in Figure 10(d), for an excitation frequency of 50 Hz, the 30 trials with a voltage of -30 V have always finished on subharmonic 3 high orbit but the 30 trials with a voltage of -70 V have almost always finished on harmonic 1 low orbit. Hence, the orbit jump is not only a question of how much energy is given to the mass but also how and when it is given.

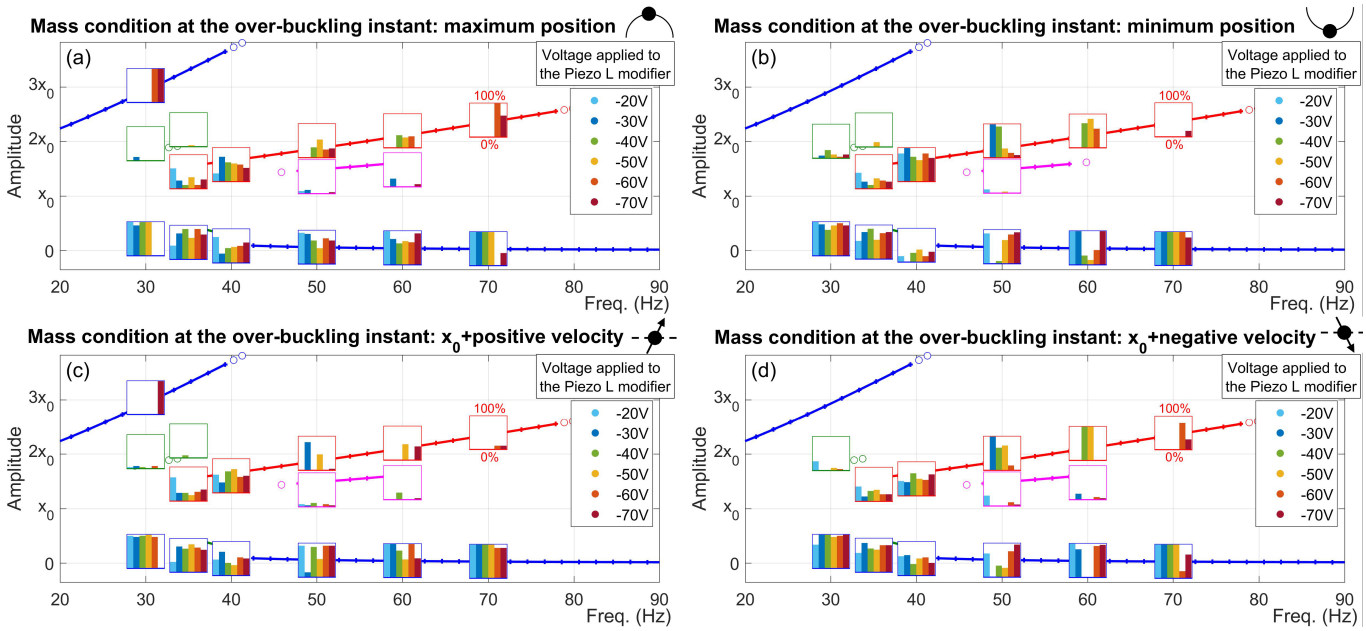

Figure 10: *Experimental results of orbit jump trials by modification of the length L showing the steady-state behaviors stabilized after the trials. Each colored stick inside the boxes corresponds to the number of trials leading to the behavior given by the position of the box. The bottom and the top of the boxes respectively correspond to 0 and 30 trials (i.e., 0% and 100% of the trials).*

(iv) The over-buckling instant plays a major role on the effectiveness of the orbit jump for a given frequency. In Figure 10 for an excitation frequency of 30 Hz, the jump from harmonic 1 low orbit to harmonic 1 high orbit is observable only for two over-buckling instants: when the mass reaches a maximum or when the mass position is x_0 with a positive velocity. Moreover, those two over-buckling instant are not identical. The first one allows an orbit jump with a voltage lower in absolute value than the second one (respectively -60 V and -70 V). These differences are probably due to the different interactions (constructive or destructive) between the excitation and the mass just after the change of length L. This interaction depends on the relative displacement of the mass with respect to the excitation which itself depends on the voltage applied to the *Piezo L modifier* and on the over-buckling instant. Hence, the most effective orbit jump will occur for a particular combination of over-buckling instant and voltage applied to the *Piezo L modifier*.

(v) It is interesting to note that, for each investigated excitation frequency, a certain combination of over-buckling instant and voltage applied to the *Piezo L modifier* leads to jump from low to high orbit for at least 70% of the 30 trials. More precisely, a certain combination leads to jump at 70% of the trials at 35 Hz and 100% of the trials for the five other frequencies. A particular combination not presented on Figure 10 was also found to ensure a jump for 100% of the trials at 35 Hz: -23 V and an over-buckling instant set when the mass position is x_0 with a positive velocity. Hence, for each excitation frequency, it is possible to find a certain combination of over-buckling instant and voltage applied to the *Piezo L modifier* leading to jump from low to high orbit for 100% of the 30 trials. Then, the possibility to change these two adjustable elements around the particular combination keeping almost 100% chance to jump depends on the stability robustness of the targeted high orbit. The more robust the targeted high orbit, the bigger the possibility to change these two adjustable elements around the particular combination keeping the highest chance to jump.

Figure 11 gathers the experimental combinations of over-buckling instant and voltage applied to the *Piezo L modifier* for which the probability to jump from low to high orbit playing with the length L is bigger than 70%. Based on these results, a few remarks can be made:

(i) Depending on the excitation frequency, several different combinations of over-buckling instant and voltage applied to the *Piezo L modifier* allows at least 70% chance to jump from low to high orbits. Their number is directly linked to the robustness of the targeted high orbit. The more robust the orbit, the bigger the number of different combinations allowing at least 70% chance to jump (*e.g.*, the maximum of robustness occurs at 40 Hz for the subharmonic 3 orbit).

(ii) This figure highlights the relevance of the chosen orbit jump strategy. Indeed, playing with the length L

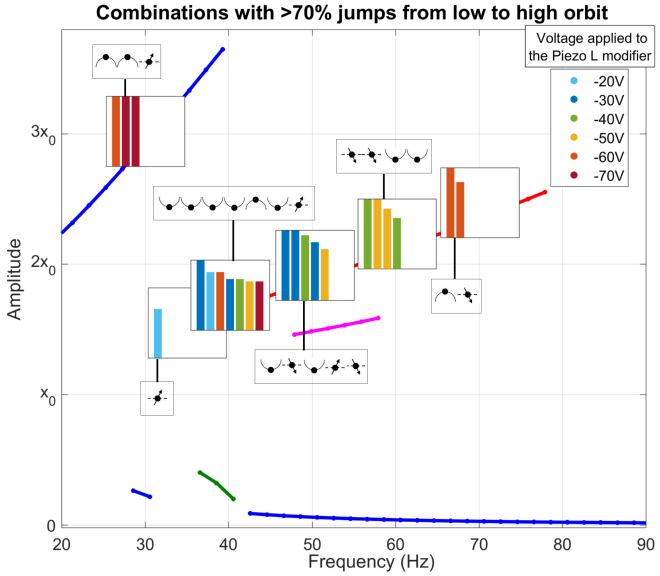

Figure 11: *Experimental combinations of over-buckling instant and voltage applied to the Piezo L modifier for which the probability to jump from low to high orbit is bigger than 70%. Each colored stick inside the boxes corresponds to the number of trials leading to the behavior given by the position of the box. The bottom and the top of the boxes respectively correspond to 0 and 30 trials (i.e., 0% and 100% of the trials). The over-buckling instant for each colored stick is detailed above or under the boxes.*

allow a high probability (>70%) to jump from low to high orbits on the whole frequency range concerned by high orbits. Moreover, this high probability is ensured for several different combinations of over-buckling instant and voltage applied to the *Piezo L modifier* depending on the robustness of the targeted high orbit.

A second way to present the experimental results is shown in Figure 12. The quantity of information plotted in this figure is the same as the one plotted in Figure 10 but presented in a different way. It shows directly the probability to jump on a high orbit after the 30 trials depending on the excitation frequency, on the voltage applied to the *Piezo L modifier* and on the over-buckling instant (the squares with black edges correspond to 100% jumps). The figure particularly highlights the following interesting fact: for each excitation frequency and over-buckling instant, the highest probability to jump on a high orbit is obtained for the minimal voltage (in absolute value) which allow orbit jumps. In other words, if the voltage is too low (in absolute value), there is no chance to jump because the energy brought to the mass is not sufficient. Then, the minimal voltage (in absolute value) allowing orbit jump corresponds to the voltage with the highest probability to jump. If this voltage is increased (in absolute value) above this minimal value, the probability to jump will globally decrease.

In conclusion, the orbit jump through the modification of the length L is a strategy showing good probabilities to jump from low to high orbits (from 70% to 100% chances to jump depending on the excitation frequency), technically achievable (voltages below 100 V) and robust as the successful orbit jumps can be obtain for several combinations of its adjustable elements. Thanks to this,

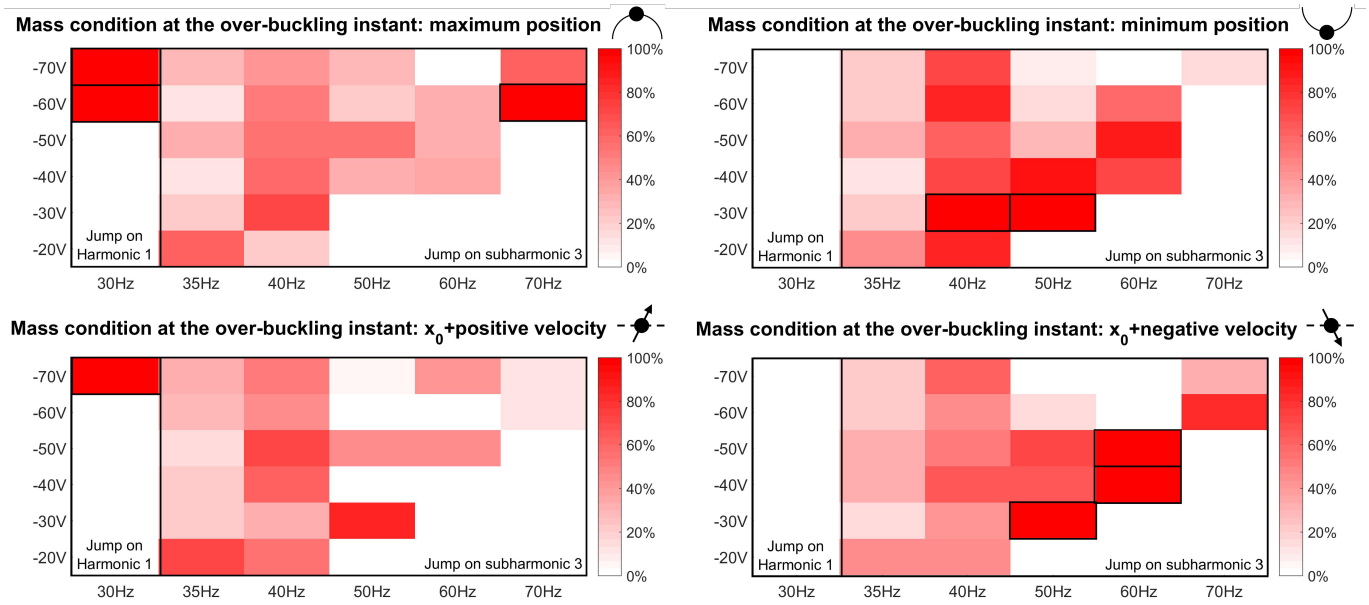

Figure 12: *Experimental results of orbit jump trials by modification of the length L showing the probability to jump on a high orbit (after 30 trials) depending on: (i) the voltage applied to the Piezo L modifier (ii) the excitation frequency (iii) the over-buckling instant. The squares with black edges correspond to 100% jumps.*

a steady-state high orbit is ensured for the bistable harvester prototype on a continuous band of 50 Hz (from 20 Hz to 70 Hz).

IV.4. Energetic considerations

The good probabilities to jump from low to high orbits is however not enough to fully assess the efficiency of the orbit jump through the modification of the length L. Hence, its energetic balance has to be taken into account. Figure 13 first recalls the experimental combinations of over-buckling instant and voltage applied to the *Piezo L modifier* allowing at least 70% chance to jump from low to high orbits already shown in Figure 11. A new experimental data is then detailed for each combination for taking into account the energy aspect: the time that the bistable harvester needed to harvest the energy which had been used to jump. It corresponds to the time needed to obtain a positive energetic balance after the trial. For each combination, this time has been averaged over all the successful orbit jump trials leading to a high orbit (among the 30 trials). The energy used to jump corresponds to the energy brought to the mass during the trial (elastic potential energy). This energy does not take into account the *Piezo L modifier* efficiency. Indeed, this study does not focus on optimizing this particular solution but focuses exclusively on the useful energy that must actually be input. However, it can be noted that in the actual configuration, the real energy consumption with our particular solution was measured to be about five times larger than the energy brought to the mass.

To compute this time, two data have to be measured: the energy provided to the mass during the orbit jump trial and the mean power harvested by the bistable harvester after the orbit jump trial during the steady-state high orbit. The latter is directly measured with the voltage across the resistance plugged to the *Piezo harvester* ($P = v_{\text{rms}}^2 / R$). The energy provided to the mass during the orbit jump trial is calculated adding the jump of potential energy at the over-buckling instant and the jump of potential energy at the over-buckling release instant (see Figure 4(b) for a numerical example). The elastic potential energy of the system as a function of time is obtained through the measurement of the mass position

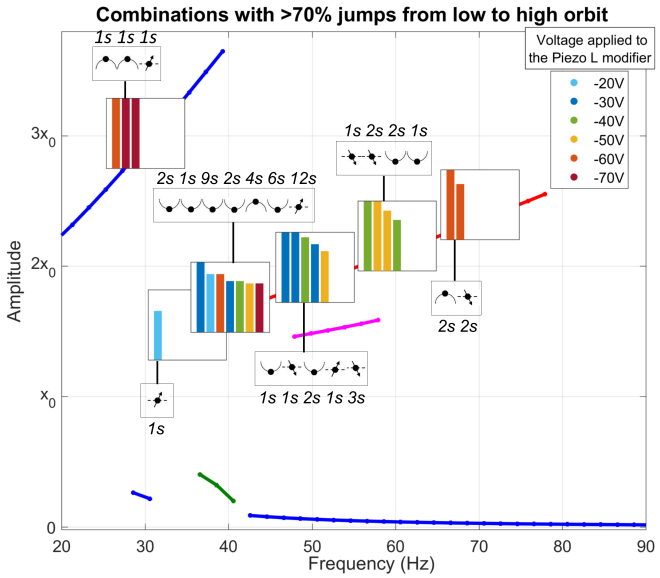

Figure 13: *Experimental combinations of over-buckling instant and voltage applied to the Piezo L modifier for which the probability to jump from low to high orbit is higher than 70% and their respective time needed to obtain a positive energetic balance (ratio between the energy provided to the mass during the trials and the mean harvested power during the following high orbit steady-states).*

x and the measurement of x_0:

$$E_{\text{potential}}(t) = \frac{\omega_0^2}{8}\left(\frac{x^4}{x_0^2} - 2x^2 + x_0^2\right) \quad (3)$$

The instantaneous variations of the latter is calculated from the variations of length L itself calculated from the variations of the voltage applied to the *Piezo L modifier* (proportional relationship).

Figure 13 shows that the time needed to obtain a positive energetic balance after the successful orbit jump trials is in the order of a few seconds (from 1 to 12 seconds depending on the high orbit reached and the voltage applied to the *Piezo L modifier* used). As reference, the time needed to obtain a positive energetic balance on the low orbit at 50 Hz varies from 50 seconds for -20 V to 15 minutes and 40 seconds at –70 V. This result confirms that the energy needed for the orbit jump playing with the length L is in the order of magnitude of the energy harvested by the bistable harvester per seconds (the power) on high orbits.

V. Conclusion

In nonlinear energy harvesters, high orbits are coexisting with low orbits (*i.e.*, low harvested energy) on a major portion of their frequency range and are thus not automatically reached. This work hence introduced different strategies to experience orbit jumps from low to high orbits playing with different parameters of the bistable harvester. The most technically achievable strategy adopted for the experimental analysis is the orbit jump with fast modifications of its buckling level. First the bistable harvester is quickly over-buckled at a particular instant and then quickly released to its initial buckling level when the mass reaches a maximum of displacement (in order to maximize the potential energy brought to the mass). Two elements of this strategy were adjustable: the amplitude of the buckling level variation and the instant at which this change starts. The results showed that choosing a good combination of those two elements leads to a high probability to jump from low to high orbits on the whole frequency range concerned by high orbits (from 70% chance to 100% chance to jump depending on the excitation frequency). Moreover, this strategy is technically achievable (the voltages applied to change the buckling level are under 100 V) and robust as the successful orbit jumps can be obtained for several combinations of its adjustable parameters. Finally, the energy needed for the orbit jump is in the order of magnitude of the energy harvested by the bistable harvester for a few seconds on the targeted high orbits. Hence the orbit jump by changing the buckling level of the bistable harvester is a relevant strategy to make sure that it reaches a high orbit in realistic conditions whenever it is possible.

Acknowledgment

The authors acknowledge the support of Région Auvergne-Rhône-Alpes through the ARC 4 Energies program.

References

[1] C. Wei and X. Jing. A comprehensive review on vibration energy harvesting: Modelling and realization. *Renewable and Sustainable Energy Reviews*, 74:1–18, 2017.

[2] C.B. Williams and R.B. Yates. Analysis Of A Micro-electric Generator For Microsystems. *Sensors and Actuators A: Physical*, 52:8–11, 1996.

[3] C.R. Mcinnes, D.G. Gorman, and M.P. Cartmell. Enhanced vibrational energy harvesting using nonlinear stochastic resonance. *Journal of Sound and Vibration*, 318:655–662, 2008.

[4] A. Erturk, J. Hoffmann, and D.J. Inman. A piezomagnetoelastic structure for broadband vibration energy harvesting. *Applied Physics Letters*, 94:128–130, 2009.

[5] R.L. Harne and K.W. Wang. A review of the recent research on vibration energy harvesting via bistable systems. *Smart Materials and Structures*, 22:23001, 2013.

[6] C. Lan and W. Qin. Enhancing ability of harvesting energy from random vibration by decreasing the potential barrier of bistable harvester. *Mechanical Systems and Signal Processing*, 85:71–81, 2017.

[7] W. Yang and S. Towfighian. A Hybrid Nonlinear Vibration Energy Harvester. *Mechanical Systems and Signal Processing*, 90:317–333, 2017.

[8] A.J. Sneller, P. Cette, and B.P. Mann. Experimental investigation of a post-buckled piezoelectric beam with an attached central mass used to harvest energy. *Proceedings of the Institution of Mechanical Engineers*, 225:497–509, 2011.

[9] S.C. Stanton, B.A.M. Owens, and B.P. Mann. Harmonic balance analysis of the bistable piezoelectric inertial generator. *Journal of Sound and Vibration*, 331:3617–3627, 2012.

[10] T. Huguet, A. Badel, and M. Lallart. Exploiting bistable oscillator subharmonics for magnified broadband vibration energy harvesting. *Applied Physics Letters*, 111:173905, 2017.

[11] T. Huguet, A. Badel, O. Druet, and M. Lallart. Drastic bandwidth enhancement of bistable energy harvesters: Study of subharmonic behaviors and their

stability robustness. *Applied Energy*, 226:607–617, 2018.

[12] A. Erturk and D.J. Inman. Broadband piezoelectric power generation on high-energy orbits of the bistable duffing oscillator with electromechanical coupling. *Journal of Sound and Vibration*, 330:2339–2353, 2011.

[13] Y.P. Wu, A. Badel, F. Formosa, W.Q. Liu, and A. Agbossou. Nonlinear vibration energy harvesting device integrating mechanical stoppers used as synchronous mechanical switches. *Journal of Intelligent Material Systems and Structures*, 25:1658–1663, 2014.

[14] C. Lan, L. Tang, and W. Qinh. Obtaining high-energy responses of nonlinear piezoelectric energy harvester by voltage impulse perturbations. *European Physical Journal Applied Physics*, 79:1–15, 2017.

[15] Y.P. Wu, J. Cao, D.J. Inman, S. Liu, W. Wang, and J. Lin. Impact-induced high-energy orbits of nonlinear energy harvesters. *Applied Physics Letters*, 106:093901, 2015.

[16] G. Sebald, H. Kuwano, D. Guyomar, and B. Ducharne. Experimental duffing oscillator for broadband piezoelectric energy harvesting. *Smart Materials and Structures*, 20:102001, 2011.

[17] G. Sebald, H. Kuwano, D. Guyomar, and B. Ducharne. Simulation of a duffing oscillator for broadband piezoelctric energy harvesting. *Smart Materials and Structures*, 20:075022, 2011.

[18] A. Masuda, A. Senda, T. Sanada, and A. Sone. Global stabilization of high-energy response for a duffing-type wideband nonlinear energy harvester via self-excitation. *Journal of Intelligent Material Systems and Structures*, 24:1598–1612, 2013.

[19] J.P. Udani and A.F. Arrieta. Efficient potential well escape for bi-stable Duffing oscillators. *Nonlinear Dynamics*, 92:1045–1059, 2018.

[20] D. Mallick, A. Amann, and S. Roy. Surfing the high energy output branch of nonlinear energy harvesters. *Physical Review Letters*, 117:197701, 2016.

[21] M.I. Dykman and M.A. Krivoglaz. Theory of fluctuational transitions between stable states of a nonlinear oscillator. *Sov. Phy. JETP*, 50:30–37, 1979.

[22] R. Almog, S. Zaitsev, O. Shtempluck, and E. Buks. Signal amplification in a nanomechanical duffing resonator via stochastic resonance. *Applied Physics Letters*, 90:013508, 2007.

[23] W.Q. Liu, A. Badel, F. Formosa, Y.P. Wu, and A. Agbossou. Novel piezoelectric bistable oscillator architecture for wideband vibration energy harvesting. *Smart Materials and Structures*, 22:035013, 2013.

[24] P.P. Friedmann. Numerical methods for determining the stability and response of periodic systems with applications to helicopter rotor dynamics and aeroelasticity. *Comp. & Maths with Appls.*, 12:131–148, 1986.

[25] R.L. Harne, M. Thota, and K.W. Wang. Concise and high-fidelity predictive criteria for maximizing performance and robustness of bistable energy harvesters. *Applied Physics Letters*, 102:053903, 2013.

[26] A. Badel and E. Lefeuvre. Nonlinear Conditioning Circuits for Piezoelectric Energy Harvesters. In E. Blokhina, A. El Aroudi, E. Alarcon, and D. Galayko, editors, *Nonlinearity in Energy Harvesting Systems Nonlinear*, pages 321–359. Springer, Cham, 2016.